

# Effect of bath temperature and concentration of buffer salt on the optoelectronic characteristics of CdS thin films synthesised by chemical bath deposition method

Zahra Makhdoumi Kakhaki, Amirali Youzbashi, Parvaneh Sangpour, Nima Naderi, Asghar Kazemzadeh

Semiconductor Department, Materials and Energy Research Center, P.O. Box 14155-4777, Karaj-Iran

E-mail: zahramakhdoomi@yahoo.com

Published in Micro & Nano Letters; Received on 12th October 2015; Accepted on 1st December 2015

CdS thin films were deposited onto glass substrate by the chemical bath deposition method, using cadmium chloride ( $\text{CdCl}_2$ ) as a source of cadmium, thiourea ( $\text{CS}(\text{NH}_2)_2$ ) as a source of sulphur, ammonium nitrate ( $\text{NH}_4\text{NO}_3$ ) as buffer salt and ammonia as pH controller and complexing agent. The effects of the deposition temperature and the concentration of ammonium nitrate on the structural, compositional, optical and optoelectrical properties of CdS thin films were investigated. The optimised sample was utilised for fabrication of photodetectors. A high photosensitivity and a short response time was reported for the photodetectors based on the sample with the bath temperature of  $65^\circ\text{C}$  and concentration of ammonium nitrate of 1.5 M compare with the other samples.

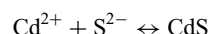
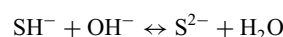
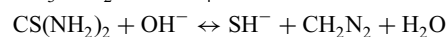
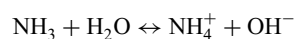
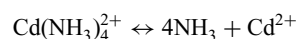
**1. Introduction:** CdS belongs to II–VI compound semi-conductor, with a direct intermediate optical band gap of 2.42 eV at room temperature, relatively low work function, and excellent thermal and chemical stability. The *n*-type semi-conductor properties of CdS is because of the intrinsic defects such as the sulphur vacancies and Cd interstitial defects. Commonly, CdS thin films are used as the buffer layer in  $\text{Cu}(\text{In,Ga})\text{Se}_2$  and CdSe solar cells and photoelectrode in photoelectrochemical cells [1–3]. CdS is a favourable material for visible light detection; it has a wide range of applications, including environmental monitoring, space research and optical communications [4]. Various techniques such as chemical vapour deposition, sputtering, molecular beam epitaxy, chemical vapour deposition, electrodeposition, spray pyrolysis, successive ionic layer adsorption and reaction, and chemical bath deposition (CBD) have been reported for the deposition of CdS thin films [5–12]. CBD is a simple and cost-effective method. However, good crystallinity is not expected if CdS is prepared at low temperatures [13]. Deposition of CdS thin films by CBD method is based on the slow release of  $\text{Cd}^{2+}$  and  $\text{S}^{2-}$  ions in an aqueous alkaline bath, utilising a complexing agent. Many authors have investigated the optoelectronic properties of CdS thin films as the buffer layer in solar cells obtained by CBD method [14–16], but few investigations have been reported on the application of CdS obtained by this method in photodetectors [17, 18].

From literatures, it can be seen that the investigation of CBD parameters such as bath temperature and concentration of buffer salt on the optoelectronic parameters of photodetectors such as response time and photosensitivity is still scanty.

In the current work, the effect of bath temperature and the concentration of buffer salt on the crystallinity, morphology, composition, optical and optoelectric properties of CdS thin films deposited by CBD method, are investigated.

**2. Experiment:** Nanocrystalline CdS thin films were deposited at alkaline bath, including cadmium chloride as a source of cadmium, thiourea as a source of sulphur, ammonium nitrate as the buffer salt which inhibit the fast release of  $\text{Cd}^{2+}$  ion, and ammonia as a pH controller and complexing agent. The possible

chemical reaction to form CdS thin films are as follows [19]



The solution was a mixture of  $\text{CdCl}_2$  (0.02 M),  $\text{CS}(\text{NH}_2)_2$  (0.5 M),  $\text{NH}_3$  (25%),  $\text{NH}_4\text{NO}_3$  (0.5 M, 1.5 M and 2.5 M) and deionised water ( $\text{DI-H}_2\text{O}$ ). The pH of solution was adjusted and fixed to 9.5 by adding  $\text{NH}_4\text{OH}$ . The pH of solution was monitored by using a pH metre in order to prevent the white precipitation of  $\text{Cd}(\text{OH})_2$ . Commercial glass slides were used as the substrates and were cleaned in acetone and isopropyl alcohol ultrasonically. Two sets of samples were prepared in this solution. The first set of films was prepared with a fixed bath temperature of  $65^\circ\text{C}$  with various concentration of ammonium nitrate from 0.5 to 2.5 M (a1, a2 samples). There was no thin film with suitable quality in the sample deposited with concentration of ammonium nitrate of 2.5 M because of the very slow release of Cd ion. However the second set of films was prepared with a fixed concentration of ammonium nitrate of 1.5 M and at varied bath temperature of  $65^\circ\text{C}$  and  $85^\circ\text{C}$  (a2, a3 samples). Thiourea ( $\text{CS}(\text{NH}_2)_2$ ) was added dropwise to the solution under continuous stirring. The cleaned glass substrates were then fixed vertically in the beakers. For better uniformity and for utilising the obtained thin films in photodetectors, the deposition repeated three times. Morphological, compositional and structural properties of the deposited thin films were studied using field emission scanning electron microscopy (FE-SEM, MIRA3 TESCAN) with energy dispersive X-ray spectroscopy (EDX, TESCAN) and X-ray diffraction (XRD, Siemens D500) using an X'Pert Pro MRD diffractometer (PANalytical Company) system equipped with Cu K $\alpha$ -radiation ( $k = 1.54056 \text{ \AA}$ ), respectively. The roughness of thin films was determined by atomic field microscopy (AFM, Auto Probe CP). The optical properties were determined by the optical

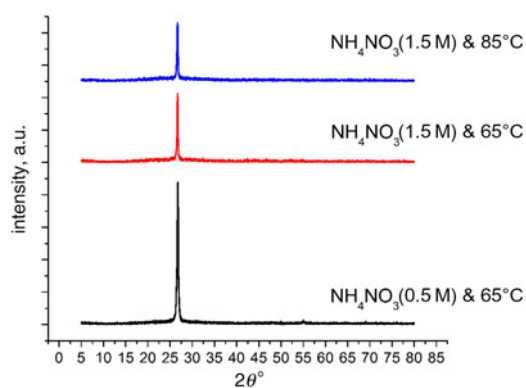


**Fig. 1** XRD patterns of CdS thin films deposited at different bath temperature and different concentration of ammonium nitrate

transmission, using PerkinElmer Spectrometer, LambdaIs USA UV-Vis spectrophotometer and photoluminescence spectroscopy (PL, Perkin Elmer – LS-5 with starting wavelength of 260 nm). The thickness was measured by cross-sectional SEM. Metal-semiconductor-metal (MSM) photodetectors were fabricated by metallisation of CdS thin films using Ag electrodes. The optoelectrical properties of fabricated photodetectors were characterised using current–voltage (I–V) measurements. The electrical measurements were conducted in the dark and under visible light with an intensity of 40W in the bias voltage range from –10 V to +10 V. The response time and recovery time were measured at a bias voltages of 5 V using a sourceMeter (Keithley 2410, USA) at ambient conditions.

### 3. Results

**3.1. Structural properties:** Fig. 1 shows the XRD patterns of CdS thin films. The crystallite size ( $D$ ) of nanostructures were calculated using Debye-Scherrer equation as follows

$$D = \frac{0.9\lambda}{\beta \cos \theta} \quad (1)$$

where  $\lambda$  is wavelength of Cu K $\alpha$  radiation ( $\lambda = 1.5406 \text{ \AA}$ ),  $\beta$  is the full-width at half maximum of intensity (FWHM) and  $\theta$  is the diffraction angle (in radian).

The XRD patterns of CdS thin films (Fig. 1) shows a peak located at  $2\theta = 26^\circ$  with high intensity which is related to (002)/(111) planes of hexagonal/cubic phase, thus CdS thin films have preferred orientation. The crystallites size of CdS thin films deposited at a1, a2, and a3 samples were 24, 39 and 36 nm, respectively.

The concentration of buffer salt and bath temperature control the deposition rate of thin films in CBD technique. At low concentration of ammonium nitrate of 0.5 M the binding between Cd ion and complexing agent is weaker than the one at higher concentration of ammonium nitrate of 1.5 M, thus the deposition rate is higher in former sample. With an increase in bath temperature, the deposition rate also increased because of the fast dissociation of thiourea and cadmium. It is well documented that thin film growth proceeds through three steps, the first step is nucleation,

the second step is subsequent coalescence and the third step is vertical growth. At high deposition rates, the nucleation step is fast; the nucleation sites concentration is then large. Thereafter, the nuclei size enlargement is limited and blocked by the surrounding nuclei. However, at low deposition rates, the low concentration of the nuclei sites enables the nuclei to grow and attain a larger size. Consequently, the grain size is larger in films deposited with lower deposition rate [19]. By the increase of concentration of ammonium nitrate from 0.5 to 1.5 M, the nucleation sites decreased thus the crystallite size increased. Previous reports showed that by an increase in bath temperature the crystallite size increased [20]. In current work the crystallite size decreased from 39 to 36 nm by the increase of bath temperature from 65°C to 85°C. This phenomena is because of the higher deposition rate for thin films deposited at 85°C which concluded the more nucleation site. This phenomena was reported earlier by Moualkia *et al.* [19]. In the current work, the deposition process was repeated three time and the seed layer played an important role for the nucleation site and determination of final nanocrystallites.

Table 1 shows the crystallite size of CdS thin films deposited at different bath temperatures and different concentration of buffer salt. It also determines the relationship between the structural, compositional, roughness and optical properties.

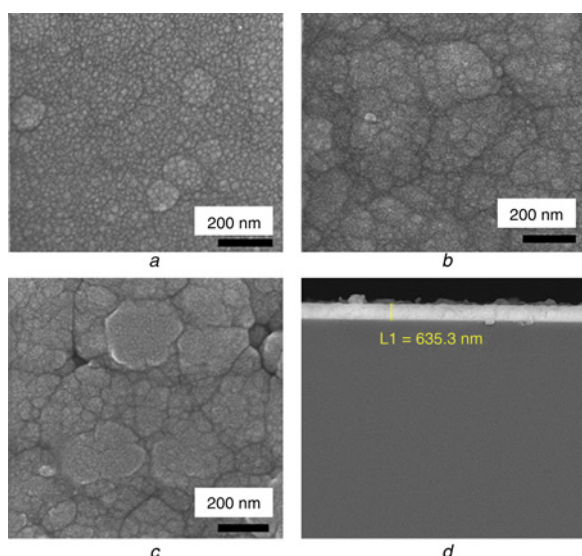
**3.2. Morphological and compositional properties:** Figs. 2a–c illustrates the FE-SEM images of CdS thin films. Fig. 2d shows the cross-sectional SEM of sample a2. According to Fig. 2a the particle size of sample a1 is smaller than the other samples and the sample a3 has the agglomerated particle. The thickness of sample a2 is about 650 nm (Fig. 2d). The thickness of sample a1 is higher than the other sample (~800 nm) which is in good agreement with the intensities in XRD patterns. It is because of the higher deposition rate. Despite of the higher deposition rate, the sample a3 has the lower thickness (~600 nm) which is attributed to the redissolve of ember by the increase of bath temperature, it is reported earlier [21]. Fig. 3 shows the EDX spectra of a1, a2 and a3 samples and the S/Cd ratio is 0.89, 0.98 and 1.015, respectively. In sample a1 the binding between Cd ion and complexing agent is weaker than the sample a2, thus the amount of Cd ion in former bath is higher than in later bath. The S/Cd ratio of sample a3 is near to the stoichiometric properties of CdS because of the fast dissociation of thiourea by the increase in bath temperature.

Fig. 4 depicts the AFM images of CdS thin films deposited at different concentration of buffer salt and different bath temperature. As shown in Fig. 4 the roughness of thin films increased as the concentration of ammonium nitrate increased from 0.5 to 1.5 M. The roughness also increased as the bath temperature increased from 65°C to 85°C. The increase in roughness could be due to the increase in the particle size [22].

**3.3. Optical properties:** The optical absorption spectra of the CdS thin films deposited at concentration of ammonium nitrate of 0.5 and 1.5 M and at different bath temperature of 65 °C and 85 °C in the UV–visible wavelength range (200–1100 nm) are presented in Fig. 5a. The Tauc plot of these samples are presented in Fig. 5b. The optical bandgap of the fabricated CdS thin films calculated from this optical data were 2.48 eV, 2.42 eV and 2.25 eV

**Table 1** Relationship between CdS thin film deposition conditions and structural, compositional, roughness and optical properties

Samples	Crystallite size, nm	FWHM	Band gap, eV	S/Cd	Roughness
NH <sub>4</sub> NO <sub>3</sub> (0.5 M) & 65 °C-a1	24	0.3250	2.48	0.89	7.5
NH <sub>4</sub> NO <sub>3</sub> (1.5 M) & 65 °C-a2	39	0.207	2.42	0.98	11.53
NH <sub>4</sub> NO <sub>3</sub> (1.5 M) & 85 °C-a3	36	0.2272	2.25	1.015	12.66



**Fig. 2** FE-SEM images of CdS thin films sample

- a a1
- b a2
- c a3
- d Cross sectional SEM of sample a2

for the a1, a2 and a3 samples, respectively. This trend is because of the change in crystallite size. The sample a3 with larger particle size and individual agglomerated grains shows the lower optical band gap. The position of absorption peak for this sample is shifted to higher wavelengths in comparison with the other samples.

The photoluminescence spectra of a1, a2 and a3 samples are shown in Fig. 6. The maximum intensity of PL spectra is in the wavelength of 460 nm which is related to the band to band region. The sample a1 has two peak in 460 nm and 680 nm which is related to band to band and sulphur vacancy region [23, 24]. The sulphur vacancy of sample a1 is because of the very fast release of Cd ion and the slow release of sulphur in comparison with cadmium. The intensity of PL spectra is related to crystallite size and thickness [25, 26]. Thus, the PL intensity of sample a1 is higher than the other thin films because of the smaller particle size and higher thickness of film. The PL intensity of sample a3

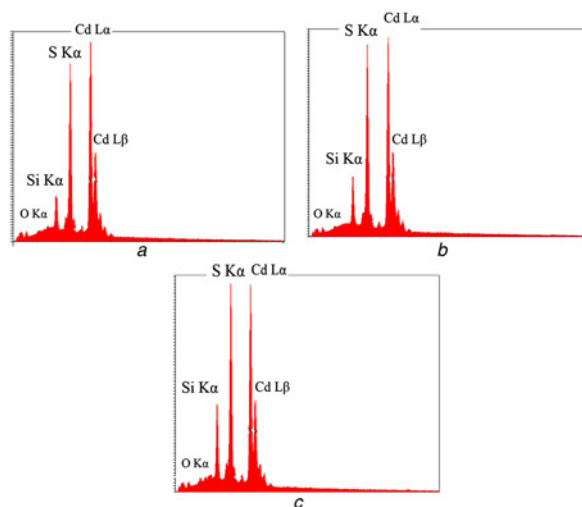


**Fig. 3** EDX spectra of CdS thin films deposited at

- a a1
- b a2
- c a3

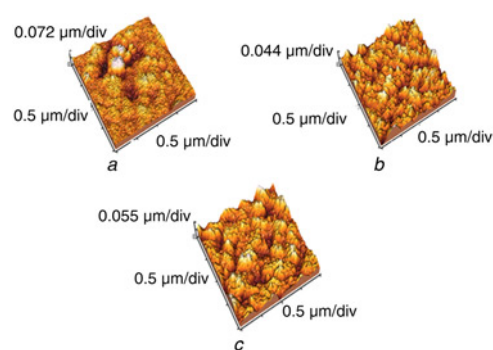


**Fig. 4** AFM images of CdS thin films deposited at

- a a1
- b a2
- c a3

is lower than the other one because of the larger particle size and smaller thickness of thin film.

**3.4. Optoelectrical properties:** The absorption of bulk CdS is mostly in visible region, thus CdS is the suitable material for visible photodetectors. At higher wavelengths, the light has insufficient energy to excite electrons for transition from valence to conduction band, which contributes to a decrease in the photocurrent. The photodetection characteristics of the fabricated Ag/CdS/Ag photodetectors were studied by measuring the  $I-V$  curves in the dark and under visible light with the intensity of 40W. The  $I-V$  characteristics showed a linear behaviour. In  $n$ -type semi-conductors, when the semi-conductor work function is greater than the metal work function, ohmic contact can be obtained [27]. The CdS work function is approximately 4.7 eV [28], which is greater than the Ag work function (4.3 eV) [29]. The obtained dark current that initiated from thermionic emission of carriers was much smaller than the photocurrent obtained upon illumination [18]. Upon illumination, the incident light excites the charge carriers from the valence band to the conduction band, and thus, the photoconductive sensitivity of the device is improved. The photosensitivity is the main factor for photodetector properties. The sensitivity was calculated using the following equation [30]

$$S = \frac{I_{ph} - I_{dark}}{I_{dark}} \times 100 \quad (2)$$

where  $I_{ph}$  is the photocurrent and  $I_{dark}$  is the dark current. Fig. 7 illustrated the  $I-V$  curves of samples at bias voltage in the range of  $-10$  V to  $10$  V. Table 2 demonstrates the dark current,

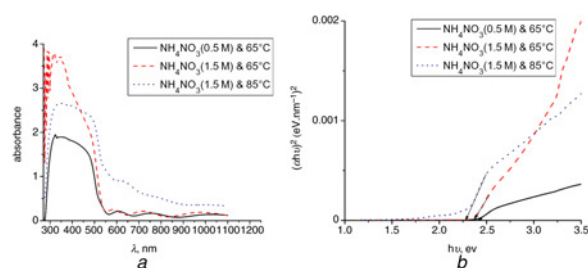


**Fig. 5** Optical absorption spectra and Tau plot of the CdS thin films deposited at concentration of ammonium nitrate of 0.5 and 1.5 M and at different bath temperature of 65 °C and 85 °C in the UV-visible wavelength range (200–1100 nm); a UV-vis spectra of CdS thin films deposited at different bath temperature and concentration of ammonium nitrate; b Tau plot of CdS thin films deposited at various bath temperature and concentration of ammonium nitrate

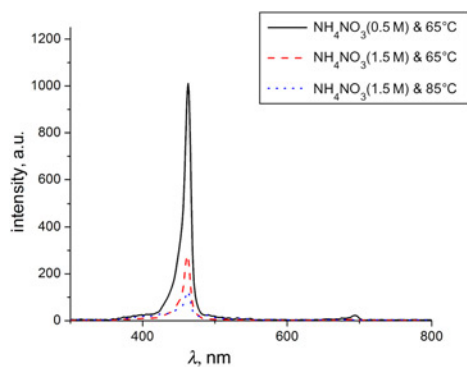


**Fig. 6** Photoluminescence spectra of a1, a2 and a3 samples

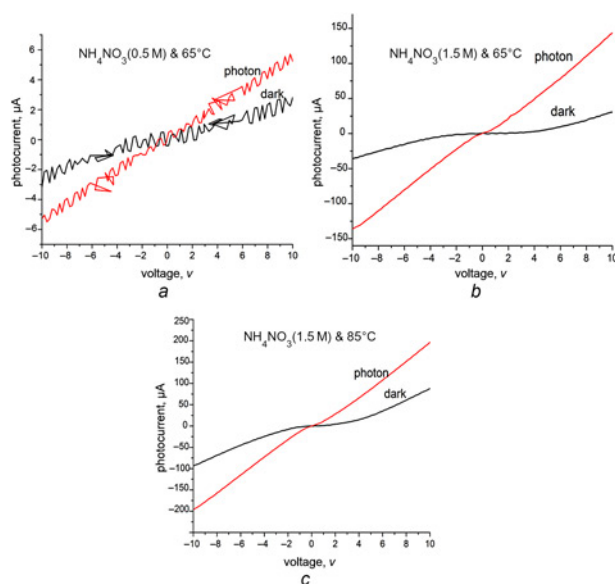


**Fig. 7** *I-V* characteristics of the fabricated Ag/CdS/Ag photodetector measured in the dark and under visible light

a a1  
b a2  
c a3

photocurrent and photosensitivity of samples fabricated by CdS thin films and Ag electrodes at applied bias voltage of 10 V which were extracted from Fig. 7. As shown in Table 2, the photosensitivity of a1, a2 and a3 samples was 84%, 369% and 123%, respectively.

The sample a1 indicated low dark current and photocurrent in comparison with the other samples because of the smaller particle size. The decrease in the particle size caused the increase in the grain boundaries. The grain boundaries act as the barrier for the electron mobility, thus the dark current and photocurrent decreased [31].

The sample a2 with the smaller particle size showed the lower dark current and photocurrent in comparison with the sample a3, but the difference between dark current and photocurrent of the

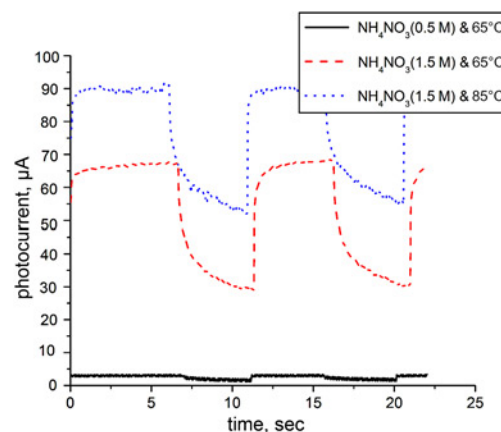


**Fig. 8** Photoresponse of the MSM CdS photodetector at bias voltage of 5 V, as illuminated by visible light

former sample is higher than the later, thus the sample a2 showed better photosensitivity.

Fig. 8 shows the photoresponse of the fabricated CdS optical sensor as a function of time at applied bias voltages of 5 V. The photocurrent rapidly increased to saturated value when the light was turned on and decreased again when the light was switched off. When the device is under illumination with enough energy, electron-hole pairs are formed and later separated under the applied electrical field at the Ag–CdS interface. One of the most important properties of a photodetector is response time, which determines the speed of a photodetector to sense an optical signal. The decay time and rise time of a1, a2 and a3 samples depicted in Table 2. Due to the high surface-to-volume ratio of sample a1 the induced defects and grain boundaries that acted as recombination centres on the surface, enhanced the free carrier recombination and shortened the decay time [32]. In comparison with a2 and a3 samples, the sample a2 showed the better response time which is related to the smaller particle size and higher amount of surface state and traps.

**4. Conclusion:** CdS thin films deposited at different bath temperature and different concentration of buffer salt in CBD bath, such as a1, a2 and a3 samples. The growth parameters affected the thin films properties such as the crystallite size, compositional, optical and optoelectrical properties. The crystallite size decreased as the nucleation sites increased. The PL peak at band to band region decreased as the crystallite size increased. The crystallite size of CdS thin films affected the photosensitivity and response speed of fabricated Ag/CdS/Ag photodetectors. The increase in the crystallite size of samples increased the photocurrent and dark current of devices and the decrease of the crystallite size enhanced the response speed due to the increase of grain boundaries and electron-hole recombination. The sample a2 with intermediated particle size, showed the higher photosensitivity and suitable response speed, thus this sample is a good candidate for visible photodetector devices.

**5. Acknowledgments:** This work was supported by Materials and Energy Research Center (MERC), Tehran, Iran (grant no. 481392055).

**Table 2** Photodetector properties of CdS thin films deposited at different bath temperature and buffer salt concentration

Samples	Darkcurrent, $\mu\text{A}$	Photocurrent, $\mu\text{A}$	Photosensitivity, %	Rise time, s	Decay time, s
a1	2.82	5.22	85	0.03	3.8
a2	30.7	144	369	0.46	3.96
a3	88.2	197	123	0.49	4.08



## 6 References

- [1] Duan H.S., Tang K.C., Hsu W.C., *ET AL.*: 'Studies of carrier recombination in solution processed CuIn(Se,S)<sub>2</sub> through photoluminescence spectroscopy', *Appl. Phys. Lett.*, 2013, pp. 102: 063902
- [2] Pérez R.M., Hernández J.A., Hernández J.S., *ET AL.*: 'Photoluminescence characteristics of CdS layers deposited in a chemical bath and their correlation to CdS/CdTe solar cell performance', *Sol. Energy.*, 2006, **80**, (6), pp. 682–686
- [3] Hilal H.S., Ismail R.M.A., Hamouz A.E., *ET AL.*: 'Effect of cooling rate of pre-annealed CdS thin film electrodes prepared by chemical bath deposition: Enhancement of photoelectrochemical characteristics', *Electrochim. Acta.*, 2009, **54**, pp. 334–337
- [4] Wei T.Y., Hung C.T., Hansen B.J., *ET AL.*: 'Large enhancement in photon detection sensitivity via Schottky-gated CdS nanowires sensors', *Appl. Phys. Lett.*, 2010, **96**, p. 013508
- [5] Ray S., Banerjee R., Barua A.K.: 'Properties of Vacuum-Evaporated CdS Thin Films', *J. Appl. Phys.*, **1889**, p. 19
- [6] Leighton W.H.: 'Electrical properties of cadmium sulfide thin films in the thickness direction', *J. Appl. Phys.*, 1973, **44**, p. 5011
- [7] Cameron D.C., Duncan W., Tsang W.M.: 'The structural and electron transport properties of CdS grown by molecular beam epitaxy', *Thin Solid Films.*, 1979, **58**, pp. 61–66
- [8] Calixto M.E., Sebastian P.J.: 'A comparison of the properties of chemical vapor transport deposited CdS thin films using different precursors', *Sol. Energy Mater. Sol. C.*, 1999, **59**, pp. 65–74
- [9] Basol B.M.: 'Electrodeposited CdTe and HgCdTe solar cells', *Sol. Cells*, 1988, **23**, p. 69
- [10] Cong H.N., Sene C., Chartier P.: 'Poly (3-methylthiophene) structural change effect on characteristics of CdS (A1): PMeT photovoltaic junction', *Energy Mater. Sol. Cells.*, 1996, **20**, p. 261
- [11] Mukherjee A., Satpati B., Bhattacharyya S.R., *ET AL.*: 'Synthesis of nanocrystalline CdS thin film by SILAR and their characterization', *Physica E: Low-dimens. Syst. Nanostruct.*, 2015, **65**, pp. 51–55
- [12] Kariper A., Güneri E., Göde F., *ET AL.*: 'The structural, electrical and optical properties of CdS thin films as a function of pH', *Mater. Chem. Phys.*, 2011, **129**, pp. 183–188
- [13] Mane R.S., Yoon M.Y., Chung H., *ET AL.*: 'Co-deposition of TiO<sub>2</sub>/CdS films electrode for photo-electrochemical cells', *Sol. Energy*, 2007, **81**, p. 290
- [14] Li H., Liu X.: 'Improved performance of CdTe solar cells with CdS treatment', *Sol. Energy*, 2015, **115**, pp. 603–612
- [15] Lin Y., Meng Y., Tu Y., *ET AL.*: 'CdS/CdSe co-sensitized SnO<sub>2</sub> photoelectrodes for quantum dots sensitized solar cells', *Opt. Commun.*, 2015, **346**, pp. 64–68
- [16] Qia J., Liu W., Biswas C., *ET AL.*: 'Enhanced power conversion efficiency of CdS quantum dot sensitized solar cells with ZnO nanowire arrays as the photoanodes', *Opt. Commun.*, 2015, **349**, pp. 198–202
- [17] Hodes G.: 'Chemical solution deposition of semiconductors films' (Marcel Dekker, Israel, 2002)
- [18] Husham M., Hassan Z., Mahdi M.A., *ET AL.*: 'Fabrication and characterization of nanocrystalline CdS thin film-based optical sensor grown via microwave-assisted chemical bath deposition', *Superlattice Microst.*, 2014, **67**, pp. 8–16
- [19] Moualkia H., Hariech S., Aida M.S., *ET AL.*: 'Growth and physical properties of CdS thin films prepared by chemical bath deposition', *J. Phys. D: Appl. Phys.*, 2009, **42**, p. 135404
- [20] Liu F., Lai Y., Liu J., *ET AL.*: 'Characterization of chemical bath deposited CdS thin films at different deposition temperature', *J. Alloy. Compd.*, 2010, **493**, pp. 305–308
- [21] Hodes G.: 'Semiconductor and ceramic nanoparticle films deposited by chemical bath deposition', *Phys. Chem. Chem. Phys.*, 2007, **9**, pp. 2181–2196
- [22] Cortes A., Gomez H., Marotti R.E., *ET AL.*: 'Grain size dependence of the bandgap in chemical bath deposited CdS thin films', *Sol. Energy Mater. Sol. C.*, 2004, **82**, pp. 21–34
- [23] Tong X.L., Jiang D.S., Li Y., *ET AL.*: 'The influence of the silicon substrate temperature on structural and optical properties of thin-film cadmium sulfide formed with femtosecond laser deposition', *Physica B.*, 2006, **382**, pp. 105–109
- [24] Mahdi M.A., Hassan J.J., Ahmed M.n.N., *ET AL.*: 'Growth and characterization of CdS single crystalline micro-rod photodetector', *Superlattices Microstruct.*, 2013, **54**, pp. 137–145
- [25] Mahdi M.A., Hassan Z., Ng S.S., *ET AL.*: 'Structural and optical properties of nanocrystalline CdS thin films prepared using microwave-assisted chemical bath deposition', *Thin. Solid. Film*, 2012, **520**, pp. 3377–3484
- [26] Ikhmayies S.J., Juwhari H.K., Ahmad-Bitar R.N.: 'Nanocrystalline CdS: in thin films prepared by the spray-pyrolysis technique', *J. Lumin.*, 2013, **141**, pp. 27–32
- [27] Wary G., Kachari T., Rahman A.: 'Comparative studies on temperature dependent I–V characteristics of Al/(p)CdTe and Ni/(n)CdS Schottky junctions and their PV effect'. AIP Conf. Proc., 2010, vol. 1249, pp. 188–191
- [28] Cui J.B., Teo K.B., Tsai J.T.H., *ET AL.*: 'The role of dc current limitations in Fowler-Nordheim electron emission from carbon films', *Appl. Phys. Lett.*, 2000, **77**, p. 183
- [29] Fischer R.S., Fischer S.N., Fauster T.: 'Image states and local work function for Ag/Pd (111)', *Phys. Rev. Lett.*, 1993, **70**, p. 654
- [30] Mahdi M.A., Hassan J.J., Ng S.S., *ET AL.*: 'Synthesis and characterization of single-crystal CdS nanosheet for high-speed photodetection', *Physica E*, 2012, **44**, pp. 1716–1721
- [31] Moualkia H., Hariech S., Aida M.S.: 'Structural and optical properties of CdS thin films grown by chemical bath deposition', *Thin Solid Films*, 2009, **518**, pp. 1259–1262
- [32] Ardakani A.G., Pazoki M., Mahdavi S.M., *ET AL.*: 'Ultraviolet photo-detectors based on ZnO sheets: the effect of sheet size on photo-response properties', *Appl. Surf. Sci.*, 2012, **256**, pp. 5405–5411